Study on Stability of Steel Strip
under the Electromagnetic Shape Controller

Atsushi Inoue

Mitsubishi Heavy Industries, Ltd. Hiroshima R&D Center, Hiroshima 733-8553, Japan
atsushi_inoue@mhi.co.jp

Hironori Fujioka

Mitsubishi-Hitachi Metals Machinery, Inc. Furnace System Group, Hiroshima 733-8553, Japan
h_fujioka@M-Hmm.co.jp

Shigeki Morii

MHI Solution Technologies Co., LTD. Maintenance Solution Engineering Department, Hiroshima 733-0036, Japan
s.morii@mhisoltech.hmw.mhi.co.jp

Mochimitsu Komori

Dept. of Applied Science for Integrated System Eng., Kyushu Institute of Technology, Kitakyushu, Fukuoka
804-8550, Japan
komori_mk@yahoo.co.jp

ABSTRACT

In a steel process line, shape controllers of steel strip using electromagnets are important devices for improving strip quality and line speed. It is confirmed that the devices are beneficial when these are applied to Continuous Galvanizing Line (CGL). However, it is necessary to avoid a static instability phenomenon by negative spring of the electromagnet, and a spill-over phenomenon by the high gain of the control system in this device. We proposed an analysis model combining the control system with the steel strip. The model was applied to a real machine to confirm the availabilities. Moreover, this paper discusses the static instability phenomenon and the spill-over phenomenon.

1. PREFACE

In the steel manufacture process line, heat-treatment and galvanizing enhance the value of the steel strip. The improvements of the quality and the operation efficiency are desired for there [1], [2].

In the Continuous Galvanizing Line (CGL) shown in Figure 1, the coating zinc weight is adjusted with wiping nozzle. The coating weight doesn't become uniform, if the cross-bowing deformation and the vibration occur on the steel strip in the wiping nozzle location, and the quality decreases. Moreover, zinc is spread more than the necessity to secure the quality, and zinc is consumed excessively. Therefore, the amount of the coating weight should be made uniform to decrease consumption of zinc. However, the steel strip just after coating cannot be supported with the roll because zinc has not coagulated, and the cross-bowing deformation is generated easily.

Then, in the wiping nozzle location where the amount of the coating weight was adjusted, we developed the steel strip shape controller that decreased the amount of the cross-bowing deformation[3]. As for this device that uses the electromagnet, the noncontact positioning and the vibration control technology that uses it by magnetic bearing and magnetic levitation are applied. It is necessary to evade static instability and spillover by using the electromagnet. The method of evading an unstable phenomenon intended for a magnetic bearing and a magnetic levitation has been studied so far[4], [5], [6]. In this report, we target the unstable oscillation generated when the steel strip is controlled by setting up this device in actual CGL. We made an analytical model by whom the steel board was combined with the system. It reports on the result of analyzing static instability and the spillover phenomenon and considering the evasion method.
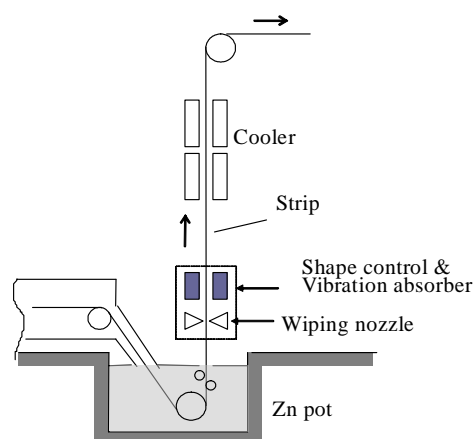

FIGURE 1: Device arrangement in CGL

2. DEVICE COMPOSITION IN STEEL MANUFACTURE PROCESS LINE

In wiping nozzle, coating zinc weight is adjusted by spraying high speed air toward the steel strip. To attempt uniform making the coated zinc by suppressing the cross-bowing of the steel strip, this device is set up in the vicinity of wiping nozzle shown in Figure 2. The specification of the device used for this analysis is shown in Table 1.

The electromagnets set up in both sides of the steel strip are driven so that this device may measure the displacement of the steel strip with the sensor, send the deflection signal with the target value to the control part, and make the steel strip follow to the target position. Moreover, this device is set up by the plural in the direction of the width of the steel strip, and the cross-bowing can be decreased.

3. ANALYSIS OF STABILITY LIMIT
3.1 Analysis model
To execute the positioning control of the steel board with stability, the analysis that unites the control system with the steel strip is done. As a result, a comprehension of the limit of stability and an unstable phenomenon are evaded.
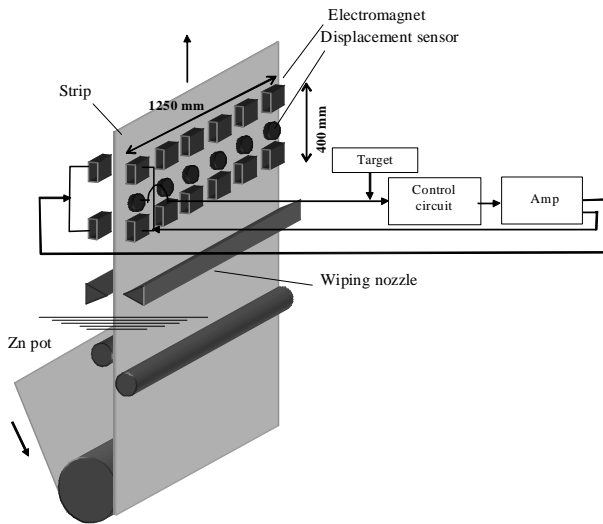
Figure 3 shows this device set up in CGL, and it is the model who let a control system combine with the steel strip which gave the tension. The model of the steel strip is regarded as tensile string, because the length (14-50m) between the roll is long enough for strip width (900-1800mm).

The action of the feedback control system that uses the electromagnet on the steel strip is modeled as a spring and a damper unit that has the frequency response. Moreover, the steel strip was modeled with geostationary. Because it is a transportation speed at which the steel strip can be influenced to the vibration characteristic by disregard though the steel strip is transported at the speed of about 100m/min in a steel manufacture line.

First of all, the steel strip to make the tension act is made the same elasticity stick and a limited element is formulated. Figure 4 assumes length l of the element and the node number at both ends to be 1 and 2, expresses the tension that acts on both ends by T, shows with the flexible volume, the rotation angle u_1, u_2, φ_1, and φ_2 at both ends, and shows the external force and the moment that acts on both ends of the element with V_1, V_2, T_1, and T_2. The motion equation of this element can be shown from these by equation (1) [7].

FIGURE 2: Device for CGL

TABLE 1: Specifications of shape control & vibration absorber

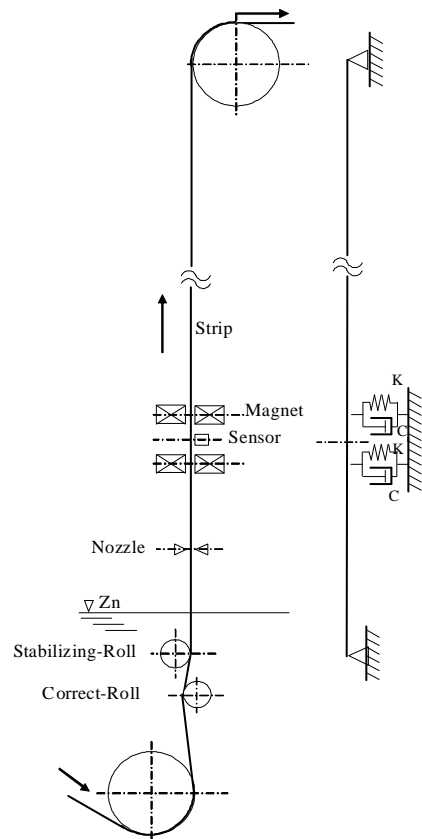| Device	Specifications
Displacement sensor	Range/volt : 25mm / 5V
Control circuit	DSP computing speed : 0.4msec
Amplifier	Rated output current : 7.2A
Electromagnet	Magnetic force : 49N/each at 3.9A Distance between Steel and Magnet :15mm

FIGURE 3: Strip model

$$[m]\{\ddot{\xi}\} + [c]\{\dot{\xi}\} + [k]\{\xi\} = \{f_\xi\} \qquad (1)$$

where

$$\{\xi\} = (u_1, \varphi_1, u_2, \varphi_2)^T$$

$$\{f_\xi\} = (V_1, T_1, V_2, T_2)^T$$

$[m]$ shows the mass procession, $[c]$ shows the damping matrix, and $[k]$ shows the rigidity procession. Respectively, equations (2)　(4) become a shown symmetric matrix.　In the steel strip that gives the tension, the rigidity by the tension is added to the rigidity procession (equation (4)) clause 2.
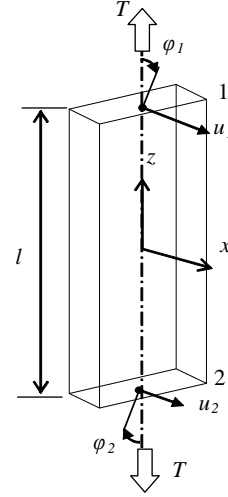

FIGURE 4: Uniform flexible beam

$$[m] = \frac{\rho A l}{(1+\varepsilon)^2}\begin{pmatrix} \frac{13}{35}+\frac{7}{10}\varepsilon+\frac{1}{3}\varepsilon^2 & & & \\ \left(\frac{11}{210}+\frac{11}{120}\varepsilon+\frac{1}{24}\varepsilon^2\right)l & \left(\frac{13}{105}+\frac{1}{60}\varepsilon+\frac{1}{120}\varepsilon^2\right)l^2 & & \\ \frac{9}{70}+\frac{3}{10}\varepsilon+\frac{1}{6}\varepsilon^2 & \left(\frac{13}{420}+\frac{3}{40}\varepsilon+\frac{1}{24}\varepsilon^2\right)l & \frac{13}{35}+\frac{7}{10}\varepsilon+\frac{1}{3}\varepsilon^2 & \\ -\left(\frac{13}{420}+\frac{3}{40}\varepsilon+\frac{1}{24}\varepsilon^2\right)l & -\left(\frac{1}{140}+\frac{1}{60}\varepsilon+\frac{1}{120}\varepsilon^2\right)l^2 & -\left(\frac{11}{210}+\frac{11}{120}\varepsilon+\frac{1}{24}\varepsilon^2\right)l & \left(\frac{13}{105}+\frac{1}{60}\varepsilon+\frac{1}{120}\varepsilon^2\right)l^2 \end{pmatrix}$$

$$+ \frac{\rho I}{(1+\varepsilon)^2 l}\begin{pmatrix} \frac{6}{5} & & & \\ \left(\frac{1}{10}-\frac{1}{2}\varepsilon\right)l & \left(\frac{2}{15}+\frac{1}{6}\varepsilon+\frac{1}{3}\varepsilon^2\right)l^2 & & \\ -\frac{6}{5} & \left(-\frac{1}{10}+\frac{1}{2}\varepsilon\right)l & \frac{6}{5} & \\ \left(\frac{1}{10}-\frac{1}{2}\varepsilon\right) & \left(-\frac{1}{30}-\frac{1}{6}\varepsilon+\frac{1}{6}\varepsilon^2\right)l^2 & \left(-\frac{1}{10}+\frac{1}{2}\varepsilon\right)l & \left(\frac{2}{15}+\frac{1}{6}\varepsilon+\frac{1}{3}\varepsilon^2\right)l^2 \end{pmatrix} \qquad (2)$$

$$[C] = \beta[k] \qquad (3)$$

$$[k] = \frac{EI}{(1+\varepsilon)l^3}\begin{pmatrix} 12 & & & \\ 6l & (4+\varepsilon)l^2 & & \\ -12 & -6l & 12 & \\ 6l & (2-\varepsilon)l^2 & -6l & (4+\varepsilon)l^2 \end{pmatrix} + \begin{pmatrix} \frac{T}{l} & 0 & -\frac{T}{l} & 0 \\ 0 & 0 & 0 & 0 \\ -\frac{T}{l} & 0 & \frac{T}{l} & 0 \\ 0 & 0 & 0 & 0 \end{pmatrix} \qquad (4)$$

Here, ρ shows the density, A shows the sectional area, I shows the geometric moment of inertia, E shows the length elasticity coefficient, ε shows the strain amount, and β shows the material damping coefficient.

According to the procedure of the finite element method, the motion equation of the entire steel strip is assembled with the use of the motion equation of each element as shown in equation (5).

$$[M]\{\ddot{X}\} + [C]\{\dot{X}\} + [K]\{X\} = \{F\} \qquad (5)$$

Here $\quad \{X\} = (u_1, \varphi_1, u_2, \varphi_2, ...)^T$

The right side of equation (5) shows the action of the external force, and the attractive force corresponding to the displacement of the steel strip is substituted in this device.

3.2 Modeling of control characteristic

The positioning control of the steel strip is executed by driving the electromagnet that sets up both sides of the steel strip through the control circuit. Figure 5 shows the block diagram of the control.

The control methods are uniting of series of *P* (proportion), *I* (integration), and the phase compensation circuit. It is the delay of the sensor and the electromagnet element, and the phase compensation circuit is installed, and, damping is given.

To show the dynamic characteristic of the control system *B(s)*, the transfer function of displacement *U(s)* and the attractive force *F(s)* that executes the Laplace transform is shown by equation (6).

$$B(s) = \frac{F(s)}{U(s)} \qquad (6)$$

The control system including the electromagnet has the following passive part characteristic and the active part characteristic for the displacement of the steel strip. The passive part characteristic $F_M(s)$ is shown by equation (7), and the steel strip is sucked to the electromagnet according to displacement regardless of the control characteristic.
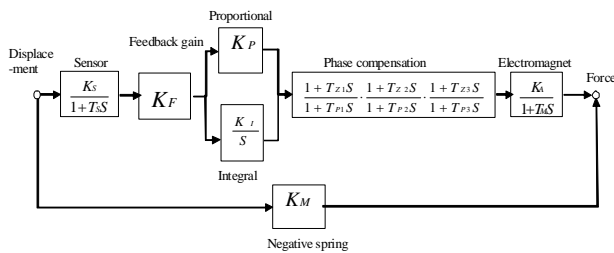
$$F_M(s) = K_M \cdot U(s) \qquad (7)$$

FIGURE 5: System and block diagram

Here, K_M [N/m] shows the passive characteristic of the electromagnet. The electromagnet is arranged on both sides of the steel strip as shown in Figure 2, and the current of the bias is applied. When the steel strip is displaced from this state as well as a magnetic bearing, force to attract the steel strip in the direction of displacement is generated, and it shows as a spring constant shown in equation (8).

$$K_M = -4 K_T \frac{i_B{}^2}{\delta^3} \qquad (8)$$

where K_T [N(m/A)^2] shows the electromagnet constant and i_B [A] shows the current of the bias. δ_g [m] shows the distance of the steel strip and the electromagnet.

Moreover, the active part characteristic can be shown by equation (9) as a transmission characteristic from the sensor of Figure 5 to the electromagnet in the sucking force that acts on the steel strip according to the displacement of the steel strip through the control system.

$$\begin{aligned} F_A(s) = &\frac{K_s}{1+T_s \cdot s} \cdot K_F \cdot \left(K_P + \frac{K_I}{s} \right) \\ &\cdot \frac{1+T_{Z1} \cdot s}{1+T_{P1} \cdot s} \cdot \frac{1+T_{Z2} \cdot s}{1+T_{P2} \cdot s} \cdot \frac{1+T_{Z3} \cdot s}{1+T_{P3} \cdot s} \cdot \frac{K_A}{1+T_M \cdot s} \end{aligned} \qquad (9)$$

Here, *K* shows the gain of the element and *T* shows the time constant. K_A [N/A] is an active characteristic of the electromagnet, and it shows by equation (10).

The electromagnet that applies the bias current is arranged on both sides of the steel strip. Active characteristic K_A for the control current to flow to the electromagnet to return the target position the steel strip when the steel strip was displaced, and is showing of the attractive force generated by this current.

$$K_A = 4 K_T \frac{i_B}{\delta} \qquad (10)$$

It is a dynamic characteristic in the control block diagram that the above shows in Figure 5.

Next, when $s = j2\pi f$ is substituted for equation (6), the complex stiffness of the control system that depends on frequency *f* can be shown by equation (11).

$$b(f) = B(j2\pi f) = b_R(f) + jb_I(f) \qquad (11)$$

Here, *R* shows a real part and imaginary part *I* is shown.

Figure 6 shows the one that the characteristic of equation (11) was drawn in Nyquist diagram. This is a attractive force characteristic corresponding to the steel strip displacement, and it substitutes for motion equation (5) of the steel strip as the external force to the steel strip through equation (6) and it is possible to show as follows.

$$[M]\{\ddot{X}\} + \left[C + \frac{1}{2\pi f} b_I(f) \right]\{\dot{X}\} \qquad (12)$$
$$+ \left[K + b_R(f) \right]\{X\} = 0$$

A static unstable phenomenon that originates in a passive characteristic of the electromagnet is generated like showing the action on the steel strip in Nyquist diagram of Figure 6 in the low frequency number region of 0.1Hz or less. The frequency domain of 0.1 20Hz is damping, and can decrease the vibration. The first element of the natural frequency of the steel strip is put in this area.

Moreover, the vibration of the steel strip by external force is decreased. It becomes an unstable region again in the high frequency region of 20Hz or more. The exciting force in this area decides by proportion and the phase compensation, is excited an innumerable natural frequency, and there is a possibility that the spillover phenomenon is generated.

In addition, passive rotation spring K [Nm/rad] that can be shown at the electromagnet position by equation (13) for the rotation angle of the steel strip is generated so that the electromagnet may have the width of limited. This influences the stability when controlling, and it adds to the rigidity procession of equation (12).

$$K_\vartheta = -\frac{1}{12} K_M \cdot d^2 \qquad (13)$$

Here, d [m] shows width in the direction of the electromagnet of the length of the steel strip.

3.3 Static stability analysis result

A static, unstable phenomenon in this device is generated when "negative stiffness of the electromagnet" is larger than "stiffness of the steel strip that gives the tension and stiffness given by the control
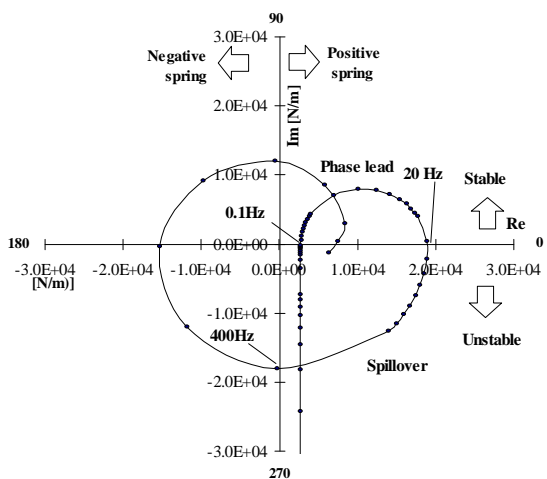
system" in the areas of the number of low frequencies shown in Figure 6. Then, the eigenvalue was analyzed by using equation (12) by the finite element method that combined the steel board with the control system [8]. In that case, the tension and the feedback gain were assumed to be a parameter.

The electromagnet of six axes is arranged in the direction of width of the steel strip, on the steel strip of 14.9m in length, 1250mm in the width, and the thickness 0.8mm, and one example of the mode of vibration analyzed by the device specification shown in Table 1 is made Figure 7. Feedback gain 0.2 is stable because of positive damping ratio and shows the mode that becomes a node at the magnet position. It is static unstable in 0.025 that lowers the feedback gain compared with this. The mode from which the steel strip is pulled to the electromagnet is shown, and the damping ratio becomes negative.

Figure 8 shows the analytical result in which the feedback gain of the control system and the tension of the steel strip are assumed to be a parameter. In the state normally controlled, it becomes a value almost equal to the natural frequency of the string that gives the tension shown in equation (14).

$$f = \frac{n}{2L} \sqrt{\frac{\sigma}{\rho}} \qquad (14)$$

Here, σ [Pa] shows the unit tension of the steel strip, ρ [kg/m^3] shows the density of the material of the steel strip, [m] shows the length of the steel strip, and shows the order of the natural frequency.

FIGURE 6: Nyquist plot
(Frequency character of feedback system)

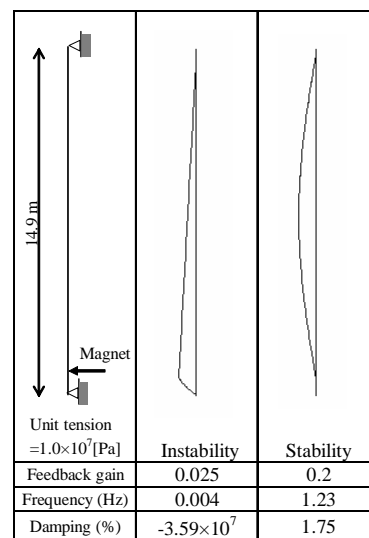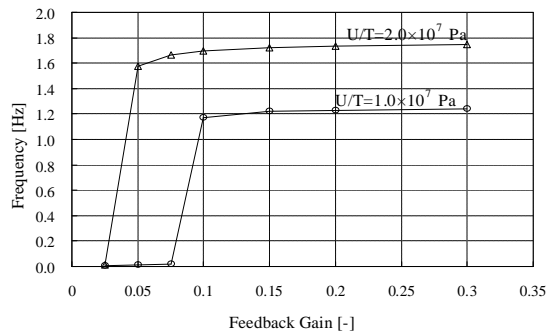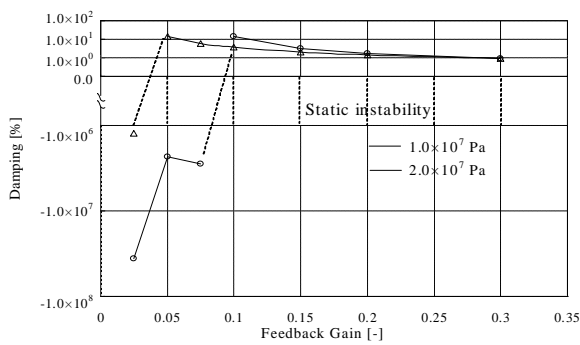| Unit tension =1.0×10^7[Pa]	Instability	Stability
Feedback gain	0.025	0.2
Frequency (Hz)	0.004	1.23
Damping (%)	-3.59×10^7	1.75

FIGURE 7: Modal analysis results static instability

(a) Natural frequency

(b) Damping ratio

FIGURE 8: Static instability analytical result

It changes from the mode of vibration of the stable state into the mode that the steel strip is attracted to the electromagnet, if the feedback gain is reduced from the state of a control normal as shown in Figure 7. The natural frequency becomes almost 0Hz, and the damping ratio indicates a negative value. In the feedback gain less than this, a negative stiffness of the electromagnet grows more than the stiffness of the steel strip and the control system, and static instability is caused. Moreover, even if the feedback gain is set low by the high tension, the steel strip is steady the tension's acting and the stiffness.

Figure 9 shows the experiment result of application to actual CGL as one example of static instability. It controls with the electromagnet of six axes in the direction of the width of the steel strip and Ch1　Ch6 is displacement of the steel strip measured with the sensor of each axis. The steel strip moves to the desired value. However, it is impossible to position with stability by having lowered the feedback gain of the control. The steel strip is attracted to the electromagnet, it comes off from the desired value, the control system operates next, the current applies to the electromagnet on the other side, and the steel strip is attracted to the electromagnet on the other side. It is an unstable phenomenon to repeat this operation. It is necessary to
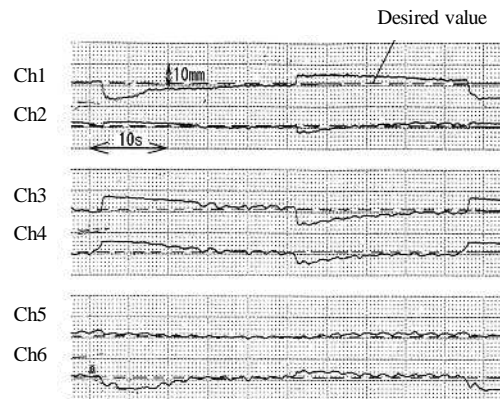

FIGURE 9: Static instability phenomena

understand the limit of stability to each tension by the analysis as shown in Figure 8, and to set the lowest value of the feedback gain for stabilization.

3.4 Dynamic stability (spillover) analytical result

The Spillover phenomenon generated by raising the feedback gain of the control system by handling the analytical model shown in Figure 3 was analyzed. Spillover is a phenomenon that the eigenvalue of the steel strip is excited by the control system in a frequency region (20Hz or more in the case of Figure 6) that is higher than the phase compensation area in the frequency character of Figure 6. Figure 10 shows the analytical result of spillover done when the steel strip condition is the same as the static stability. The 33rd eigenvalues (40.2Hz) show negative damping ratio (-0.275%), and there is a possibility of oscillating by external force. It is shown that the spillover phenomenon is generated. In the frequency region where the phase compensation area was exceeded, all eigenvalues make the damping ratio negative. However, there is a difference in the effect of excitation depending on the position of the electromagnet and the mode of vibration of the steel strip. Then, the result of plotting the negative damping maximum value of all natural frequencies is shown in Figure 11 in each feedback gain. It is understood that it becomes easy for negative damping to increase by raising the feedback gain, and to generate the spillover phenomenon. In an actual steel manufacture process line, even whenever damping acts with the steel strip and the ancillary equipment, and it becomes negative damping in the analysis, spillover is not necessarily generated. However, the generation limit in new equipment can be forecast by understanding the limit value of the measurement by one point if the relation between a feedback gain and negative damping can be quantitatively understood as shown in Figure 11.
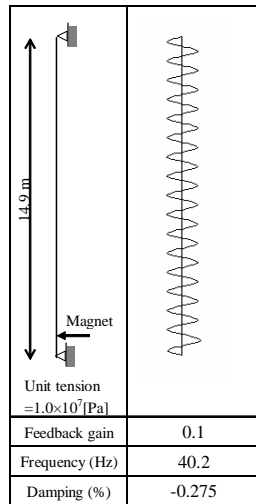
Unit tension $=1.0 \times 10^7$[Pa]	
Feedback gain	0.1
Frequency (Hz)	40.2
Damping (%)	-0.275

FIGURE 10: Modal analysis results
High-frequency instability

(a) Displacement

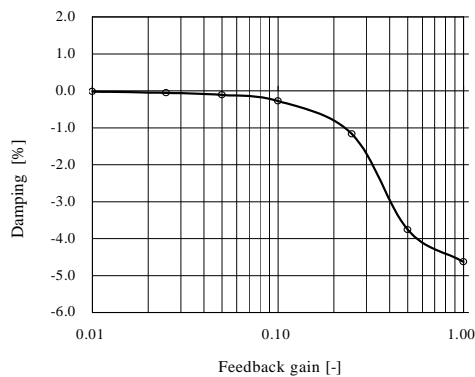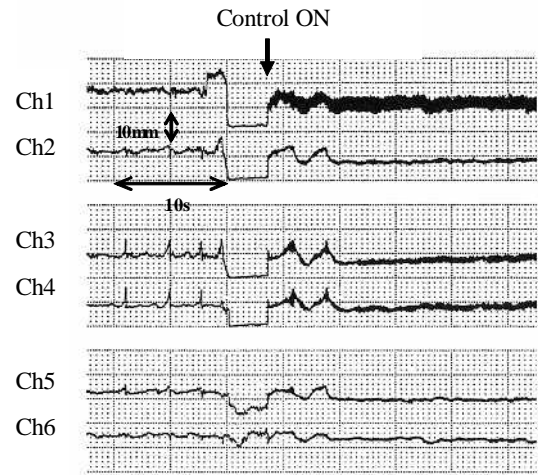FIGURE 11: High-frequency instability analytical result

(b)　Spectrum (Ch3)
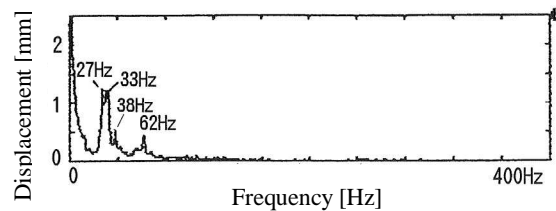
FIGURE 12: High-frequency instability phenomena

Figure 12 is an example of raising the feedback gain in an actual steel manufacture line, and causing the spillover phenomenon by feedback gain 0.2. The steel strip vibrates at the same time as the control beginning and the amplitude increases. In that case, when the frequency analysis result is seen, the eigenvalue of frequency region 27　60Hz where the phase compensation was exceeded is excited by the control system. Moreover, the damping of equipment exists in an actual steel manufacture line, and even if the analysis is negative damping, spillover is not necessarily generated. It was generated for the first time by raising the feedback gains up to 0.2 in this example.

4. APPLICATION EXPERIENCE TO CGL

When this device is applied to an actual steel manufacture line, it is necessary to operate it without causing an unstable phenomenon named static instability and spillover. The analysis shown in Chapter 3 is done, the lower bound of the feedback gain in which static instability is prevented is set, and the upper bound of the feedback gain in which spillover is prevented is set for that. Moreover, it is not necessary to examine the limit of stability when a real machine is applied because a steady control constant can be set by the design stage and to adjust the control constant. Therefore, the contact of the steel strip and peripherals by generating an unstable phenomenon (vibration) can be prevented. When this device is applied to the position shown in Figure 1, Figure 13 is a vibration of the steel strip measured with the sensor of this device. An unstable phenomenon was not generated, and was able to be operated with stability. Moreover, the result of suppressing the vibration of 200μm or less caused in the frequency band of 0.1　5Hz enough was obtained [9].

5. CONCLUSION

The unstable phenomenon generated in the shape controller of the steel strip that used the electromagnet was forecast analyzing it as follows.
(1)An analytical model by whom the steel strip was united with the control system that made the electromagnet an actuator was made.
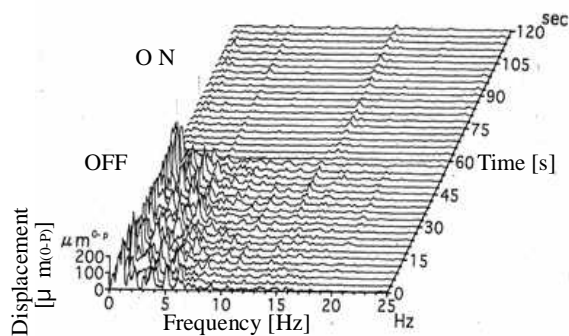
FIGURE 13: Effect of application test in CGL

(2)The generation limit of static instability was analyzed by handling an analytical model in consideration of the active part characteristic of the control system, and the passive part characteristic of the electromagnet. As a result, the relation between the generation limit and the tension given to the steel strip was clarified.

(3)The spillover phenomenon generated by raising the feedback gain of the control system was forecast by handling an analytical model. As a result, the relation between and the gain and a negative amount of damping in which the spillover phenomenon was shown was clarified.

(4)The control constant was set based on the generation limit of static instability and spillover requested by an analytical model. As a result, it was confirmed not to cause an unstable phenomenon in an actual steel manufacture line and to operate with stability.

Moreover, the steel strip with different thickness and width flows to the steel manufacture line, and the tension given to it changes, too. The vibration characteristic of each steel strip is different, and the best setting of the control constant according to it and the establishment of the method of evaluating the limit of stability are future tasks.

References

1. Andoh, A. et al., Recent Advance in Coated Steel Sheets, Tetsu-Hagane, Vol. 89, No.1, 2003, pp. 3-17.

2. Tobiyama, Y. Abotani, K. Hot-Dip Galvanized Steel Sheet with Excellent Surface Quality for Automotive Outer Panels, JFE Technical report, No.4, Nov. 2004, pp. 55-60.

3. Morii, S. et al., Study on Shape Control and Vibration Absorber of Strip in Steel Process Line, Mitsubishi Heavy Industries Ltd. Technical Review, Vol. 32, No. 2, May 1995, pp. 128-131.

4. Nonami, K. et al., Vibration and Control of a Flexible Rotor Supported by Magnetic Bearings, Transactions of the Japan Society of Mechanical Engineers, Series C, Vol. 54, No. 507, 1988, pp. 2661-2688.

5. Oshinoya, Y. et al., Electromagnetic Levitation Control of a Traveling Steel Belt, Transactions of the Japan Society of Mechanical Engineers, Series C, Vol. 57, No. 536, 1991, pp. 1246-1253

6. Hasegawa, S. Oshinoya, Y. Ishimashi, K. Basic Examination on Elastic Vibration Control of an Electromagnetic Levitation System for Thin Steel Plate, Proceeding of the Faculty of Engineering of Tokai University, Vol. 43 No. 2, 2003, pp. 59-64.

7. Kawashima, M. et al., Vibration Analysis of Rotor-Bearing Systems by Finite Element Method, Mitsubishi Heavy Industries Ltd. Technical Review Vol. 20, No. 4, July 1983, pp. 377 - 383.

8. Katayama, K. et al., Development of Rotor Dynamics Analysis System Considering Control System, Mitsubishi Heavy Industries Ltd. Technical Review, Vol. 26, No. 3 May 1989, pp. 253 - 256.

9. Morii, S. et al., Study on Shape Control and Vibration Absorber of Strip in Steel Process Line, LDIA 2005, Kobe-Awaji, Japan, Sept. 25-28, 2005, pp. 516-519.